Preparation of Gold Nanoplates by an Electrochemical Method

Min Zhou,[†] Shenhao Chen,*[†,††] Shiyong Zhao,[†] and Hongfang Ma[†]
[†]*Department of Chemistry, Shandong University, Jinan, Shandong, 250100, P. R. China*
[††]*State Key Laboratory for Corrosion and Protection, Shenyang, Liaoning, 110016, P. R. China*

(Received September 16, 2005; CL-051185)

Single-crystal triangular and hexangular nanoplates of gold can be obtained by electrochemical reducing $AuCl_4^-$ in the presence of PVP and a small amount of H_2PtCl_6. With the concentration of H_2PtCl_6 increasing from 0 to 1×10^{-3} mol/dm^3, the morphology of Au nanoparticles evolved from spheroids to triangular and hexangular nanoplates with well-defined facets.

Metal nanocrystals have drawn considerable interest in the past years because of their application to catalysis, biosensing, optics, and magnetic devices.[1,2] Silver and gold nanocrystals have been prepared by photochemical, electrochemical, biochemical, and thermochemical methods.[3–6] There are a great number of reports focusing on gold nanowires and silver nanodisks, but a small number of reports on the preparation of gold nanodisks and nanoplates in the past decade. Liz-Marzan et al., Klabunde et al., Chen et al., and Tominaga et al. prepared triangular and hexangular gold nanoplates by chemical, biological, or photoreduction method, respectively.[7–10] Tsuji et al. reported a microwave-polyol method to produce gold nanoplates stabilized by PVP.[11] Recently, Au microplates were synthesized by the reduction of $HAuCl_4$ with *o*-phenylenediamine in aqueous solution.[12] Lee et al. and Chen et al. also used triblock copolymer or liquid crystals as a template to synthesize gold nanoplates.[13,14]

Herein, we report an electrochemical procedure for preparing platelike gold nanoparticles. We added small amounts of H_2PtCl_6 to aqueous solution[15] in our foregoing electrochemical synthesis approaches. To our surprise, small amount of the additives induced a dramatic change on the morphologies of the nanoparticles. In contrast with our foregoing approaches, a great number of triangular and hexangular nanoplates instead of spheroid particles appeared in this approach. Typically, 5 mL of 1×10^{-2} M of $HAuCl_4$ solution, 20 mL of 0.1 M KNO_3, 20 mL of 10 g/L PVP solution and 5 mL H_2PtCl_6 (1×10^{-3} M) solution were mixed while stirring. The solution was purged by nitrogen. The electrochemical synthesis of gold nanoplates was performed in a simple two-electrode cell. Two $1.0 \times 1.0\,cm^2$ platinum sheets being 5 cm apart were employed to prepare the electrolysis electrodes. The electrolysis was carried out in the galvanostatic manner at room temperature under stirring. The KNO_3 serves as the supporting electrolyte, and PVP serves as the stabilizer for nanoparticles to prevent their further growth. Electrolysis was used for a typical current density of 10 mA/cm^2 and a typical electrolysis time of 30 min.

The morphology of the nanoparticles obtained was first characterized by TEM, as shown in Figure 1a. The image indicates that the nanocrystals consist of a large amount of plates, mainly triangular and hexagonal in shape. We also obtained a small quantity of by-products of spherical particles in the solutions. And the spherical particles were mainly platinum nanoparticles. Figures 1b and 1c show the representative images of triangular and hexangular nanoplates. The corresponding selected area electron diffraction (SAED) (Figures 1b and 1c inset, respectively) patterns were obtained by focusing the electron beam on the nanoplate lying flat on the TEM grid. The SAED patterns reveal that a hexagonal symmetry diffraction spot pattern is generated, demonstrating that the gold nanoplates are single crystal with a preferential growth direction along the gold {111} plane.[9] The crystallinity of the gold nanoplates was further confirmed by the corresponding XRD pattern (Figure 2). The three sharp peaks can be assigned to the {111}, {200}, and {220} diffraction peaks of gold metal, respectively, indicating that the precipitate is composed of pure crystalline gold. Referring to Figure 2, the value of the Au lattice constant has been estimated to be $a = 4.0760$ Å, a value which is consistent with $a = 4.0768$ Å reported by the JCPDS file No. 4-0784.[16] Also mentioned is that the intensity of the {111} plane is much higher than the other lattice planes. This indicates that {111} plane of gold nanoplates tend to be preferentially oriented parallel to the surface of the supporting substrate. This structure feature is quite common for the metal nanoplates, such as gold plates.[9]

High-resolution TEM was used to further investigate the crystal structure of the nanocrystals. Figure 3 shows a typical HRTEM image of the corner of an individual nanoplate. The image shows lattice fringes with the interfringe distance measured to be 2.40 Å, which corresponds well with the lattice spacing of the {111} the planes (2.39 Å). The chemical compo-

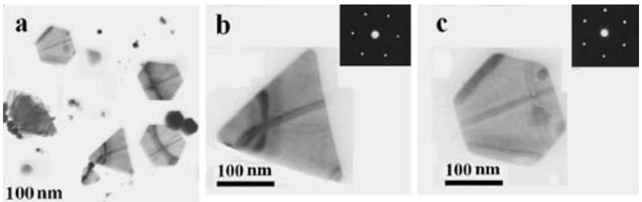

Figure 1. (a) TEM image of gold nanoplates prepared by electrolysis reduction with added H_2PtCl_6 (1 mM). (b, c) Representative TEM images and corresponding SAED patterns (inset) of the triangular and hexangular gold nanoplates as-prepared, respectively.

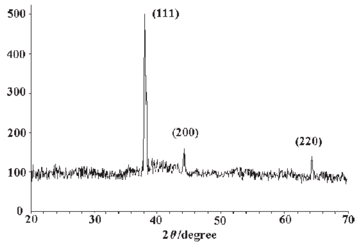

Figure 2. XRD pattern of a typical sample as-prepared.

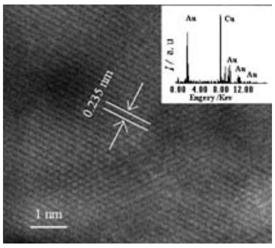

Figure 3. HRTEM and EDAX (inset) from the vertex of one of the triangular gold nanoplate.

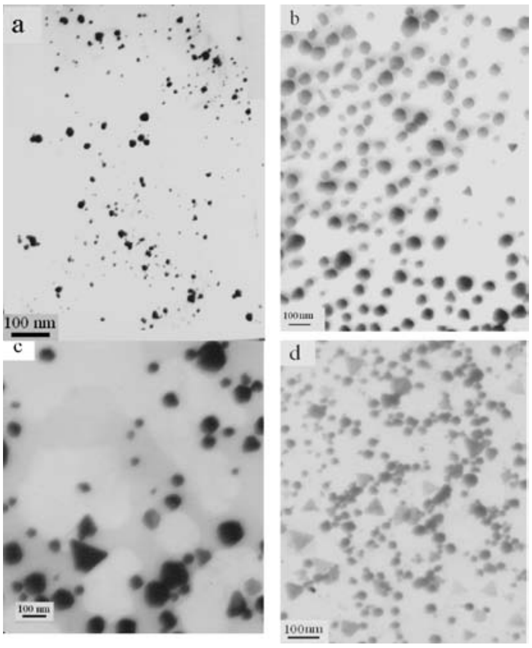

Figure 4. TEM images of gold products synthesized in the absence of H_2PtCl_6 (a) and in the presence of H_2PtCl_6, 0.1 mM (b), 0.5 mM (c), 1 mM (d).

sition of the particles was further determined by energy-dispersive X-ray analysis (EDAX). The EDAX (Figure 3 inset) obtained from the nanoparticles only shows the peaks corresponding to Au, thus indicating that the particles are pure metallic Au (the peak of Cu comes from Cu grids).

In this synthesis, the use of added H_2PtCl_6 was critical to the formation of gold nanoplates. When no H_2PtCl_6 was added, we only obtained a wine red colloidal gold solution. Figure 4a shows a typical TEM image of the gold product obtained in the absence of H_2PtCl_6, under otherwise identical conditions. Clearly, the resulting gold product mainly consists of small spherical nanoparticles with no platelike structure in shape. Upon an increase of the H_2PtCl_6 concentration to 0.1 mM, some triangular nanoplates (Figure 4b) appear coexisting with dominating spherical nanoparticles. When the H_2PtCl_6 concentration became 0.5 mM, more platelike gold nanocrystals appear (Figure 4c). When the concentration of H_2PtCl_6 was increased to 1.0 mM, there are much more and larger equilateral or truncated triangles and hexagons with the edge size (Figure 4d). When H_2PtCl_6 rises to 10 mM, a large number of precipitates are produced and particles hardly can be observed. However, it is not clear at the present time how H_2PtCl_6 influences the growth of different crystal plans of gold nanoplates and the detailed mechanism requires further investigation.

In this paper, single crystal triangular and hexagonal gold nanoplates were easily synthesized in solution through the addition of H_2PtCl_6 to a conventional electrochemical synthesis. In contrast to our previous work, we consider that H_2PtCl_6 plays an important role in the forming process of the platelike structure. It is believed that large-scale shape-controlled gold nanoparticles will be conveniently produced through further optimization of this synthetic process and expected to find intriguing applications in field such as catalysis, biosensor, recording media, and optics.

This work was performed under the auspices of the National Nature Science Foundation of China (No. 20373038)

References

1 V. F. Puntes, K. M. Krishnan, and A. P. Alivisatos, *Science*, **291**, 2115 (2001).
2 J. F. Wang, M. S. Gudiksen, X. F. Duan, Y. Cui, and C. M. Lieber, *Science*, **293**, 1455 (2001).
3 R. C. Jin, Y. W. Cao, C. A. Mirkin, K. L. Kelly, G. C. Schatz, and J. G. Zheng, *Science*, **294**, 1901 (2001).
4 Y. Yu, S. Chang, and C. R. C. Wang, *J. Phys. Chem. B*, **101**, 6661 (1997).
5 S. S. Shankar, A. Rai, B. Ankamwar, A. Singh, A. Ahmad, and M. Sastry, *Nat. Mater.*, **3**, 482 (2004).
6 J. U. Kim, S. H. Cha, K. Shin, J. Y. Jho, and J. C. Lee, *Adv. Mater.*, **16**, 459 (2004).
7 N. Malikova, I. Pastoriza-Santos, M. Schierhorn, N. A. Kotov, and L. M. Liz-Marzan, *Langmuir*, **18**, 3694 (2002).
8 S. I. Stoeva, B. L. V. Prasad, S. Uma, P. K. Stoimenov, V. Zaikovski, C. M. Sorensen, and K. J. Klabunde, *J. Phys. Chem. B*, **107**, 7441 (2003).
9 Y. Zhou, C. Y. Wang, Y. R. Zhu, and Z. Y. Chen, *Chem. Mater.*, **11**, 2310 (1999).
10 D. Ibano, Y. Yokota, and T. Tominaga, *Chem. Lett.*, **32**, 574 (2003).
11 M. Tsuji, M. Hashimoto, Y. Nishizawa, and T. Tsuji, *Chem. Lett.*, **32**, 1114 (2003).
12 X. Sun, S. Dong, and E. Wang, *Angew. Chem., Int. Ed.*, **43**, 6360 (2004).
13 J. U. Kim, S. H. Cha, K. Shin, J. Y. Jho, and J. C. Lee, *Adv. Mater.*, **16**, 459 (2004).
14 L. Wang, X. Chen, J. Zhan, Z. Sui, J. Zhao, and Z. Sun, *Chem. Lett.*, **33**, 720 (2004).
15 M. Zhou, S. H. Chen, H. P. Ren, L. Wu, and S. Y. Zhao, *Physica E*, **27**, 341 (2005).
16 P. Bayliss, "Mineral Powder Diffraction File Date Book," JCPDS, Swarthmore, PA (1986).

Published on the web (Advance View) November 19, 2005; DOI 10.1246/cl.2005.1670